Astron. Astrophys. 347, 249–257 (1999)

ASTRONOMY AND ASTROPHYSICS

Activity cycle and surface differential rotation of the single Pleiades star HD 82443 (DX Leo)

S. Messina[1], **E.F. Guinan**[2], **A.F. Lanza**[3], **and C. Ambruster**[2]

[1] Istituto di Astronomia, Università di Catania, Viale A.Doria 6, I-95125 Catania, Italy
[2] Astronomy and Astrophysics Department, Villanova University, Villanova, PA 19085, USA
[3] Osservatorio Astrofisico di Catania, Viale A.Doria 6, I-95125 Catania, Italy

Received 3 November 1998 / Accepted 29 March 1999

Abstract. The results of a long-term photometric monitoring of the young Pleiades moving group member HD 82443 are presented. A sequence of fifteen optical light curves obtained from 1989 to 1998 confirms the presence of a rotational modulation with a mean period of 5.377 days attributable to cool photospheric spots. The Maximum Entropy and the Tikhonov regularization criteria have been applied to compute maps of the photospheric spot pattern. They show that the total spotted area is subject to cyclic changes as large as $\sim 10\%$ of the star's surface with a mean period of 3.89 yr.

The seasonal photometric period shows variations correlated with the phase of the activity cycle, which can be interpreted as the result of a migration of the starspots in latitude over a differentially rotating star. The dependence of the photometric period on the cycle phase is opposite that of the Sun and similar to those observed in HD 114710 and HD 10476. A lower limit for the amplitude of the differential rotation in latitude can be estimated to be $\frac{\Delta\Omega}{\Omega} \simeq 0.04$.

Nearly simultaneous UV observations obtained in 1991 show the presence of chromospheric and transition region plages which do not seem to be in close spatial association with the photospheric spots.

Key words: stars: activity – stars: chromospheres – stars: individual: HD 82443 – stars: late-type – stars: rotation – stars: starspots

1. Introduction

HD 82443 (= DX Leo = Gl 354.1; K0V; $V \simeq 7.02$ mag; $B-V = +0.76$, $P_{rot} = 5.377$ d) is a single, main-sequence star with strong chromospheric and transition-region line emissions and an optical flux modulation which can be attributed to dark photospheric spots, coming into and out of view as the star rotates (Soderblom 1985, Messina & Guinan 1996, Kazarovets & Samus 1997).

It is a high proper motion star with a relatively large parallax of $\pi = 56.35$ mas (Perryman 1997). High precision radial velocity measurements carried out within the CORAVEL program show HD 82443 to have a constant radial velocity of $v_r = +8.2 \pm 0.24\,\mathrm{km\,s^{-1}}$, thus indicating that it is probably not a member of a close binary system (Duquennoy et al. 1991). Independent radial velocity measures obtained by Griffin (1994) yield a mean value of $v_r = +8.9 \pm 0.5\,\mathrm{km\,s^{-1}}$ and also show no indication of variability.

The projected rotational velocity of HD 82443 has been measured by Benz & Mayor (1984) finding: $v \sin i = 6.0 \pm 1.0\,\mathrm{km\,s^{-1}}$, while Soderblom (1995, priv. comm.) estimates a slightly larger value: $v \sin i = 7.0 \pm 2.0\,\mathrm{km\,s^{-1}}$ and Fekel (1997) gives: $v \sin i = 6.2 \pm 0.8\,\mathrm{km\,s^{-1}}$.

Soderblom & Clements (1987) pointed out that HD 82443 has space velocity components ($U = -14$, $V = -24$, $W = -1\,\mathrm{km\,s^{-1}}$) that are very close to those of the Pleiades star cluster ($U = -9, V = -29, W = -12\,\mathrm{km\,s^{-1}}$) suggesting that it is likely to be a member of the Pleiades moving group with an age of about 70 Myr. The implied young age of HD 82443 and the short rotation period are consistent with the observed high levels of chromospheric and transition region emissions and fit well the *Activity-Period-Age* relashionship for single late-type stars (Soderblom & Clements 1987).

The chromospheric emission in the Ca II H&K lines has been monitored by Baliunas et al. (1995, 1996a) who report the detection of a rotational modulation with a period of ~ 6 d and suggest a possible activity cycle with a period of 2.8 ± 0.1 yr.

Recent studies of optical light curves were published by Henry et al. (1995a), who determined a photometric period of 5.43 ± 0.03 d, and Strassmeier et al. (1997) who studied the rotational modulation and the long-term trend of the average optical flux.

In the present paper we discuss previously published and new optical photometry for the entire 1989–1998 period, thus filling the gap in the data sequence of Strassmeier et al. (1997). The good time coverage allows us to find evidence for a short-term activity cycle and to measure the variation of the rotation period of the spots versus the cycle phase, presumably related to the latitudinal migration of the active regions over the surface of the differentially rotating star along the activity cycle.

Moreover, we present UV observations performed by IUE which may help to constrain the non-thermal energy output of

Send offprint requests to: S. Messina (sme@sunct.ct.astro.it)

the star's atmosphere, complementing data recently obtained in the EUV and X-ray spectral domains (cf. Lampton et al. 1997).

2. Observations

2.1. Optical photometry

The photometric observations of HD 82443 presented in this paper have been collected from 1989 through 1998, using two Automated Photometric Telescopes (APT, see Boyd & Genet 1986): a) the Phoenix-10 APT having an aperture of 25 cm, in 1989; and b) the "Four College Consortium" APT, with an aperture of 75 cm, during the 1990–1998 period. All the observations were made with standard U, B and V filters using HD 82191 (A0V; $V = 6.64$[1]; $B - V = +0.08$) as the comparison star and HD 81146 (K5III; $V = 4.46$; $B - V = +1.22$) as the check star. Ten second integrations were used and the usual observing sequence *sky-comparison-check-variable-comparison-sky* was employed. The observations were corrected for atmospheric extinction and the instrumental differential magnitudes were converted into the standard UBV system. Because of the close angular separation between the variable, the comparison and the check star, atmospheric corrections were always very small. The transformation into the standard system is made with an accuracy of the order of 0.01, 0.01, and 0.02 mag in the V magnitude, B−V and U−B color indexes, respectively. No significant light variations were detected from the differential measures of comparison and check star, indicating that the light of the comparison star stayed constant within about ± 0.015 mag.

The data collected in the 1989 observing season have been already presented in a previous paper (Messina & Guinan 1996) and are reported here to perform a study of the long-term spot evolution of HD 82443. Our complete set consists of ten observing seasons of data each of which has been analysed using a Scargle-Press period search routine to derive the period of the photometric modulation during the given time interval (Scargle 1982, Horne & Baliunas 1986). In Table 1 we report the date range, the number of observations N_m, the photometric period P and its uncertainty ΔP as derived by means of the method of Horne & Baliunas (1986), the semiamplitude A of the fitting sinusoid of the optical modulation and the *false-alarm-probability* (FAP) of the peak frequency. This last quantity estimates the probability a peak of that height could result from a similar sample of Gaussian noise with the same variance of the analysed data (cf. Horne & Baliunas 1986). A search for secondary periodicities during each season has also been performed by filtering the primary frequency modulation from the data and recomputing a periodogram for the residual data according to the prescription of Horne & Baliunas (1986) and Baliunas et al. (1995). However, in none of the ten seasons we have found significant evidence for secondary periodicities in the optical modulation up to a FAP of 5%, when the primary frequency is assumed to be real.

[1] This value of magnitude from HIPPARCOS photometry updates the previous one adopted in Messina & Guinan (1996).

Table 1. Seasonal information and photometric modulation of HD 82443 (see the text for explanation).

Date range HJD−2440000	N_m	$P \pm \Delta P$ (days)	A	FAP (%)
7567–7664	191	5.412±0.004	0.033	$< 10^{-8}$
8346–8362	65	5.303±0.110	0.012	$5.0\ 10^{-5}$
8622–8702	110	5.360±0.008	0.027	$< 10^{-8}$
9050–9103	118	5.417±0.017	0.018	$< 10^{-8}$
9284–9329	87	5.478±0.048	0.009	$2.0\ 10^{-3}$
9441–9488	140	5.248±0.027	0.011	$5.0\ 10^{-5}$
9738–9814	313	5.359±0.005	0.027	$< 10^{-8}$
10084–10109	273	5.426±0.016	0.027	$3.4\ 10^{-2}$
10437–10520	176	5.440±0.011	0.015	$< 10^{-8}$
10813–10882	125	5.451±0.009	0.027	$< 10^{-8}$

The photometric period turns out to be significantly variable from season to season with a mean value of $\langle P \rangle = 5.377 \pm 0.073$ d over the entire data interval. It has been adopted in the ephemeris used to compute the phases of the light curves analysed in the present study:

$$HJD = 2447573.78 + 5.377 \times E \quad (1)$$

where E is the number of rotation periods elapsed from the first observed light minimum at HJD=2447573.78.

The light curves of HD 82443 showed remarkable variations in shape and amplitude over different time scales. The shortest-term variability can be attributed to optical flaring, whereas the variability observed on time scales of a few rotations may be attributed to sizeable intrinsic changes of the photospheric spot pattern. It proved possible to select fifteen time intervals along which the flux showed a regular modulation which could be attributed to the rotation of a stationary spot pattern on the photosphere of the star. In such a way, fifteen light curves were obtained with typical standard deviations of the normal points of about 1% in the B and V bands and about 2% in the U band. An optical flare occurred around phase 0.49 in the 1992.05 light curve, but the corresponding point was removed from the light curve to avoid systematic errors in the subsequent modelling.

The main characteristics of the analysed light curves are reported in Table 2. In the present study we shall model only the V-band light curves because the information on spot geometry contained in the simultaneous U and B light curves is basically the same.

2.2. UV spectroscopy

In late 1991, almost at the same time of our photometric monitoring, we observed HD 82443 with the IUE satellite, searching for a short-term variability at UV wavelengths and its possible correlation with the visual light variation. The star was observed both with long (LWP) and short wavelength (SWP) primary cameras once per day along one rotation period. A local background continuum was derived on both sides of each observed line and its interpolated value at the centre of the line was subtracted to obtain the net integrated line flux. The fluxes

Table 2. Mean epochs, number of observing nights, mean V-band magnitudes, colour indices and peak-to-peak amplitude of the light curves of HD 82443.

Epoch	1989.18	1989.32	1991.34	1992.05	1992.18
# nights	38	33	13	13	9
V	7.06	7.05	7.04	7.08	7.07
$U-B$	0.32	0.30	0.33	0.35	0.33
$B-V$	0.76	0.76	0.78	0.77	0.78
ΔU	0.13	0.13	0.05	0.09	0.11
ΔB	0.09	0.09	0.03	0.07	0.09
ΔV	0.08	0.08	0.03	0.06	0.08
Epoch	1993.24	1993.87	1994.30	1994.88	1995.11
# nights	19	17	23	12	16
V	7.04	7.03	7.05	7.07	7.07
$U-B$	0.34	0.41	0.38	0.42	0.42
$B-V$	0.77	0.72	0.77	0.77	0.75
ΔU	0.06	0.04	0.05	0.07	0.11
ΔB	0.05	0.04	0.05	0.05	0.09
ΔV	0.05	0.03	0.04	0.05	0.08
Epoch	1995.22	1995.99	1997.01	1997.08	1998.08
# nights	18	18	14	23	26
V	7.07	7.09	7.07	7.06	7.05
$U-B$	0.40	0.39	0.33	0.32	0.33
$B-V$	0.75	0.76	0.79	0.79	0.79
ΔU	0.10	0.09	0.07	0.11	0.14
ΔB	0.09	0.07	0.05	0.07	0.08
ΔV	0.08	0.07	0.04	0.06	0.08

were corrected for the sensitivity degradation (Teays & Garhart 1990) and transformed into surface fluxes (erg cm^{-2} s^{-1}) adopting the conversion factor $\frac{F}{f} = 9.69217 \times 10^{17}$, computed from the Barnes-Evans relations, using the magnitude V=7.08 and the color index $B-V = +0.77$ obtained from the simultaneous optical photometry (Barnes & Evans 1976).

Before 1991, HD 82443 had already been observed with the IUE satellite in 1983 and 1984 in both SWP and LWP cameras. We reanalysed those spectra, applying a reduction procedure consistent with that adopted for the 1991 data, in order to investigate possible long-term changes of the chromospheric and transition region emissions.

The ultraviolet surface net fluxes obtained for HD 82443 are reported in Table 3. Their relative uncertainties are < 20–25%, except for CI and HeII which have uncertainties $> 30\%$ because of the lower signal-to-noise ratio at shorter wavelengths.

3. Analysis of the optical data

A map of the spot distribution on HD 82443 can be derived by an analysis of the rotational modulation of the optical flux, but the solution is not unique due to the low information content of the wide-band light curves. In order to obtain a unique and stable solution, we need to assume a regularization criterion, i. e., to introduce some a priori constraint on the properties of the photospheric map. In the present approach, two kinds of regularization criteria shall be adopted: a) the Maximum Entropy method (ME); and b) the Tikhonov criterion (T), which are described in detail by, e.g., Cameron (1992).

The star's surface is divided into elements (pixels) of $9^\circ \times 9^\circ$ extension. The specific intensity of the i-th pixel varies as a function of the fraction f_i of its surface covered with spots (*spot filling factor*). More precisely, if I_u is the specific intensity of the unspotted photosphere of the i-th pixel, and $I_s = C_s I_u$ that of its spotted photosphere, the specific intensity of the pixel I_i will be:

$$I_i = f_i I_s + (1 - f_i) I_u \tag{2}$$

where the brightness contrast C_s is assumed to be constant and $0 \leq f_i \leq 1$. The unspotted photospheric intensity changes over the star's surface according to the usual linear relationships for limb-darkening and gravity-darkening (see Kopal 1959).

The map of the filling factor which fits a given light curve is obtained by finding the distribution of the f_i's which gives a constrained extremum of the Maximum Entropy or the Tikhonov functionals, respectively, subject to a given χ^2 limit, set according to the accuracy of the observations. A detailed description of the adopted procedure, including a discussion of the sources of error and the accuracy, can be found in Lanza et al. (1998).

In the present models we have adopted a mean effective temperature $T_{eff} = 5370$ K for the unspotted photosphere and $T_{spot} = 4300$ K for the spotted photosphere, deriving C_s in the black-body approximation (cf. Messina & Guinan 1996). The inclination of the rotation axis relative to the line of sight has been assumed $i = 60^\circ$, derived from the mean rotation period of 5.377 days, the measured $v \sin i \simeq 6.0$ km s^{-1} and an estimated stellar radius of 0.85 $R_\odot$. The relative difference between polar and equatorial radii $(R_e - R_p)/R_e = 5.9 \cdot 10^{-5}$ has been computed after Kopal (1959), whereas the limb-darkening coefficient in the V band, $u_V = 0.72$, has been taken from Diaz-Cordovès et al. (1995) and the gravity-darkening coefficient has been assumed $\nu = 0.25$. The unspotted V magnitude has been chosen as the brightest observed in the 1989–1998 period, i. e., $m_V = +7.013$ at HJD 2450877.8376 (rotation phase 0.4798). The optimal values of the Lagrange multipliers and the corresponding values of the χ^2 as defined in Lanza et al. (1998), have been reported in Table 4 for the light curves of our sequence. A sample of our final light curve fits together with the corresponding maps of the filling factor in Mercator projection, are shown in Fig. 1 for the Maximum Entropy solutions and in Fig. 2 for the Tikhonov solutions, respectively.

As discussed in detail in Lanza et al. (1998), our regularized maps should be regarded as an *intermediate step* of the analysis and used only to derive quantities which do not depend on the regularizing criterion adopted, e.g., the distributions of the spots vs. longitudes, their change in time and the variations of the total spotted area.

The variations of the total spotted area vs. time appear to be very similar for both Maximum Entropy and Tikhonov solutions (see Fig. 3b). The systematic difference between the values of the area obtained with the two regularizing criteria are due to their different a priori assumptions on the properties of the spot pattern, whereas the accuracy of the *variation* of the area versus

Table 3. Integrated surface net fluxes of chromospheric and transition region lines obtained from IUE spectra at low and high resolution; phases are reckoned according to Eq. (1). Epochs are expressed in modified Julian days: MJD = HJD−2440000.

Image	Epoch	Date	Phase	Exp.	Flux (10^5 erg cm^{-2} s^{-1})			
number	(MJD)			(s)	CII	CIV	HeII	CI
SWP43397LLG	8606.7722	12.16.91	0.118	6000	0.947	1.453	1.127	1.396
SWP43405LLG	8607.7708	12.17.91	0.304	6000	0.943	1.277	2.150	1.478
SWP43413LLG	8608.7736	12.18.91	0.490	6600	1.256	1.969	0.906	1.228
SWP43423LLG	8609.7805	12.19.91	0.678	6600	0.495	1.234	0.768	1.688
SWP43433LLG	8610.8305	12.20.91	0.873	6599	1.160	1.571	0.754	1.580
SWP43437LLG	8611.7646	12.21.91	0.046	7200	1.024	1.743	1.130	1.752
					MgII k		MgII h	
LWP22002HLG	8606.8389	12.16.91	0.131	4800	17.31		14.17	
LWP22023HLG	8608.8423	12.18.91	0.503	4200	20.51		16.40	
LWP22031HLG	8609.8458	12.19.91	0.689	3900	18.79		14.81	
LWP22035HLG	8610.7652	12.20.91	0.860	3900	19.42		15.06	
LWP22042HLG	8611.8389	12.21.91	0.061	4620	17.49		14.57	
	Long-term activity				CII	CIV	HeII	CI
SPW19488LLG	5709.4576	01.10.84		25200	0.971	1.541	1.139	1.520
					MgII k		MgII h	
LWP2106HLG	5608.8611	10.22.83		7800	–		1.946	
LWP2586HLG	5709.4576	01.10.84		2400	21.65		19.18	

Table 4. The Lagrangian multipliers and the χ^2 of the light curve fits with ME and T regularizing criteria, respectively.

Mean Epoch	λ_{ME}	χ^2_{ME}	λ_T	χ^2_T
1989.18	3.0	0.163	80.0	0.132
1989.32	3.0	0.660	80.0	0.642
1991.34	3.0	0.127	80.0	0.084
1992.05	3.0	0.201	80.0	0.155
1992.18	3.0	0.107	80.0	0.078
1993.24	3.0	0.109	80.0	0.080
1993.87	3.0	0.146	80.0	0.125
1994.11	3.0	0.119	80.0	0.098
1994.88	3.0	0.161	80.0	0.117
1995.11	3.0	0.734	80.0	0.416
1995.22	3.0	0.190	80.0	0.169
1995.99	3.0	0.199	80.0	0.170
1997.01	3.0	0.098	80.0	0.066
1997.08	3.0	0.235	80.0	0.207
1998.08	3.0	0.388	80.0	0.357

time is about 1% for both ME and T models (cf. Lanza et al. 1998).

The total spotted area resulting from the modelling can be considered as the sum of two components, one uniformly distributed in longitude (A_U), the other non-uniformly distributed (A_D), respectively. A periodogram analysis revealed a periodicity of $P_{cyc} = 3.89 \pm 0.03$ yr in the total area for the ME solutions and $P_{cyc} = 3.72 \pm 0.03$ yr for the T solutions with a FAP of 0.25% in both cases. From the plots in Figs. 3a and 3b we see that more than two complete cycles are covered by the observations with activity minima occuring at about 1990.5, 1994.0, 1998.0, and maxima at about 1992.0 and 1996.0. The component of the spot area distributed unevenly in longitude shows a cycle with a shorter period of 2.62 ± 0.03 yr for the ME solution and 2.62 ± 0.03 yr for the T solutions with a FAP of 0.15% in both cases. It is interesting to analyse the entire photometric data set to search for other possible long-term periodicities which may not be apparent in the modulation of the spot areas on the seasonal time scale and to obtain an independent confirmation of the existence of an activity cycle. The periodogram of the entire photometric data set is shown in Fig. 4 for the $3.0 \cdot 10^{-4} - 3.0 \cdot 10^{-3}$ d^{-1} frequency range. Three frequencies show a power exceeding a FAP of 0.1%. However, the peak at frequency $\omega_2 = 5.22 \cdot 10^{-4}$ d^{-1}, turns out to be an alias of the primary peak at frequency $\omega_1 = 7.04 \cdot 10^{-4}$ d^{-1}, because it disappears after filtering the primary frequency from the data (cf. Fig 4b). We conclude that only two frequencies are present in the long-term photometric data set: a) the primary frequency ω_1, which corresponds to the periodicity already found in the spot total area with a period of 3.89 ± 0.03 yr and FAP $< 0.1\%$, and b) a frequency $\omega_3 = 1.04 \cdot 10^{-4}$ d^{-1}, which corresponds to the period of 2.62 yr shown by the unevenly distributed component of the spot area, with FAP$= 5\%$ in the hypothesis that the primary frequency is real (cf. Horne & Baliunas 1986). The Scargle-Press method gives a higher significance for such two periodicities when applied to the entire photometric data set than when applied to the area values derived from the light curve modelling, because the number of data is much larger in the first case. However, in both cases the statistical significance of the results is high, with the spot modelling providing us with

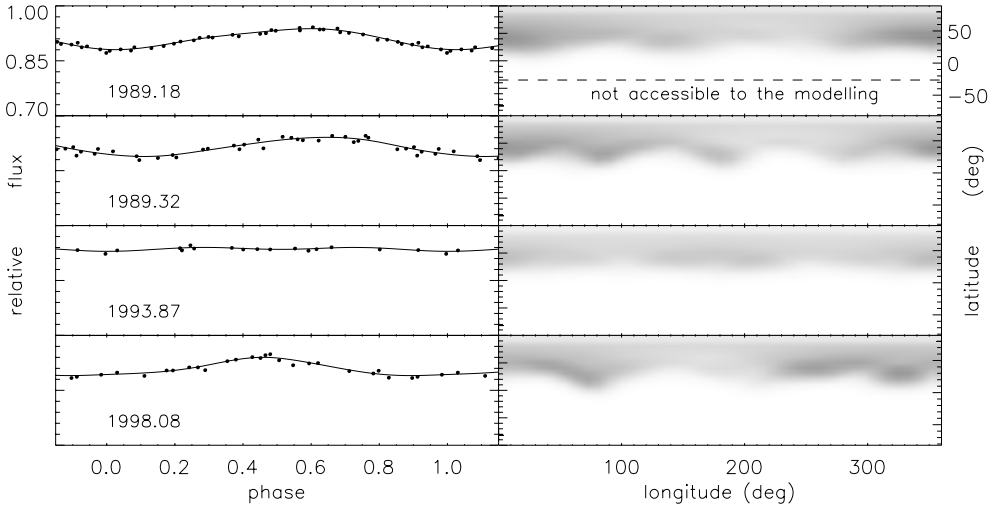

Fig. 1. Some of the V-band light curves of the analysed sequence (filled circles) fitted by the Maximum Entropy spot models (continuous lines). The mean epoch of each light curve is indicated in the corresponding plot, respectively. The flux is in relative units, with unity corresponding to the adopted unspotted magnitude. Phases are computed according to Eq. (1). The distributions of the spot filling factor are shown on the maps in the right hand panels, respectively. The longitude increases in the direction opposite to the stellar rotation, in such a way that the phase at which a given pixel crosses the central meridian is equal to its longitude. Spots located at latitudes below -30° can not contribute to the flux, because the star's rotation axis is inclined by 60°, and therefore those latitudes are not accessible to the modelling.

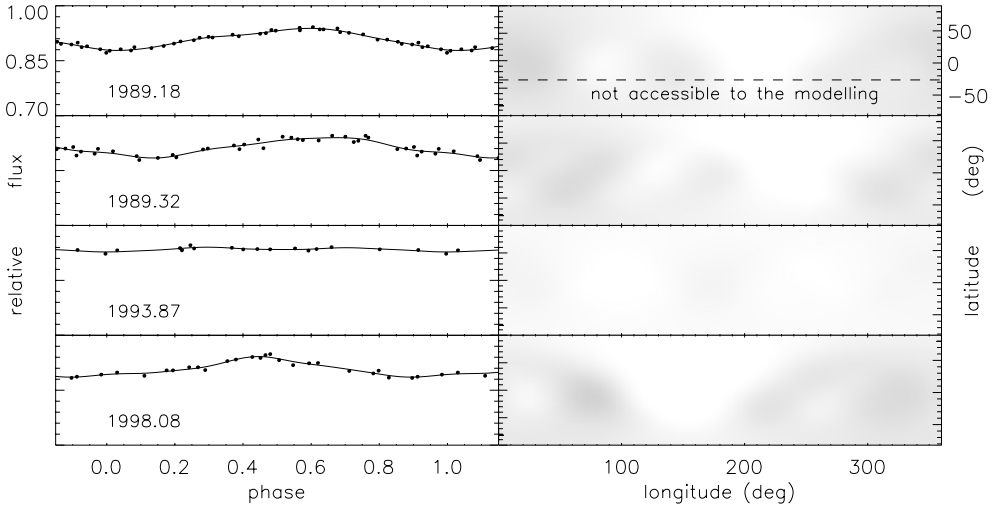

Fig. 2. The same V-band light curves of Fig. 1 (filled circles), fitted by the Tikhonov spot models (continuous lines). The flux is in relative units, with unity corresponding to the adopted unspotted magnitude. Phases are computed according to Eq. (1). The corresponding distributions of the spot filling factor are shown on the right hand panels, respectively. The same reference frame of Fig. 1 has been adopted.

additional information on which kind of spot area component is responsible for the different periodicities.

The activity level as measured by the total spotted area is correlated with the photometric period determined in Sect. 2, as shown in Fig. 3e. We clearly see that the photometric period steadily increases from a minimum of ~ 5.25 d at the 1990.5 activity minimum up to a maximum of ~ 5.45 d at the next minimum in 1994.0, then jumps back to ~ 5.25 d at the beginning of the new cycle and begins to increase again along that cycle. Such a behaviour may be interpreted in terms of a migration of the main latitude of the spot activity along the activity cycle on a differentially rotating star as will be discussed in Sect. 5. In the framework of such a hypothesis, a lower limit for the amplitude of the surface differential rotation can be derived from the observed range of the photometric period and turns out to be $\Delta\Omega/\Omega \simeq 0.04$. It is lower than the value of the solar surface differential rotation, but in good agreement with the value derived by the relationship provided by Henry et al. (1995b) for a sample of active spotted stars.

The distributions of the spotted area vs. longitude are plotted in Fig. 5 for the maps obtained according to the Maximum Entropy and Tikhonov criteria, respectively. The actual longitude resolution of the present solutions is between 50° and 70°, whereas the uncertainty in the relative spot area per longitude bin is between 10% and 40% for both regularization criteria. Such estimates have been derived by the analysis of several simulated light curves (see Lanza et al. 1998).

In Fig. 5 we can see that the longitudes of the maximum and the minimum of the distributions appear to be similar for both regularization criteria and do not depend on the kind of regular-

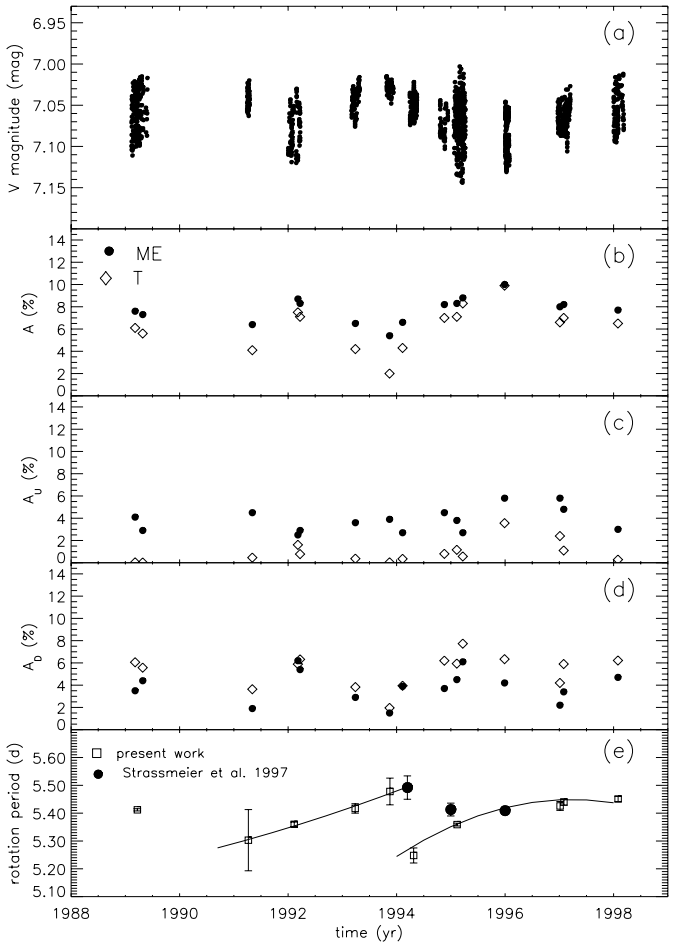

Fig. 3. a Light variations of HD 82443 in the years from 1989 through 1998. **b** Total spotted area vs. time for the ME (filled circles) and T solutions (open diamonds), respectively. The area unit is the photospheric area of the star. **c** Area of the spot component distributed evenly in longitude vs. time for the ME and the T solutions, with the same symbols as in panel **b**, respectively. **d** The same plot for the unevenly distributed component of the spot pattern. **e** The photometric period with error bars as determined from periodogram analysis. Solid lines are parabolic fits to the data. Filled circles are determinations by Strassmeier et al. (1997).

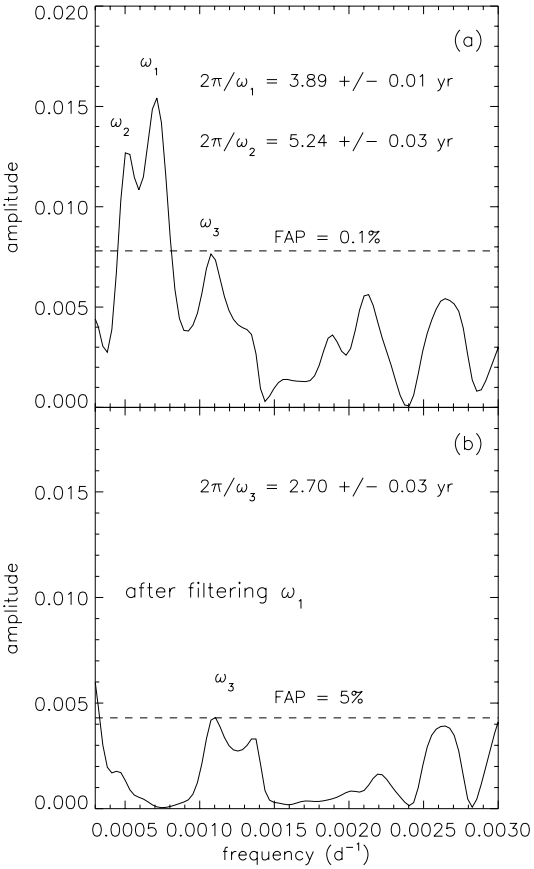

Fig. 4. a The periodogram of the entire photometric data set with the indication of the significant frequencies (see the text). **b** The periodogram of the residual data obtained after filtering the modulation with frequency ω_1 from the initial data.

ization adopted because they are directly related to the minimum and maximum of the corresponding light curves, respectively.

Usually two longitudes of maximum spottedness are present, separated by $\sim 150^\circ - 180^\circ$, but occasionally patterns with one or three active longitudes may be observed. The longitudes change versus time as a consequence of the rearranging of the spot pattern and the variation of the rotation period of the spots along the activity cycle. Typical lifetimes for the active longitudes may be estimated from the sequence of plots in Fig. 5 and appear to be of the order of a few hundred days.

4. Analysis of the UV data

The integrated line fluxes show a short-term modulation with peak-to-peak amplitudes ranging from $\sim 18\%$ for the chromospheric lines up to $\sim 60\%$ for the transition region lines (see Table 3 and Fig. 7). A plot of the line flux vs. rotation phase shows that chromospheric and transition region fluxes correlate fairly well with each other with the exception of CI and HeII fluxes. Their low amplitude modulations are likely to be spurious because of the higher uncertainty of their flux values (see Sect. 2.2).

The above results may be interpreted as evidence for the presence of bright plages in the outer atmosphere of HD 82443, unevenly distributed in longitude and whose visibility is modulated by stellar rotation. Chromospheric and transition region plages appear to be in closely spatial association.

In order to compare the plage distribution with that of the photospheric spots, the nearly simultaneous 1992.05 V-band light curve is also plotted together with the line fluxes in Fig. 7. Although the photometric coverage in phase is not complete, the minima in the optical continuum and in the line fluxes appear to be near in phase, whereas the maxima are separated by a phase lag of $\Delta\phi \simeq 0.3 = 108^\circ$. Such a result suggests that the spatial association between starspots and chromospheric and transition region plages may not be close on HD 82443. However, it is also possible that the maximum in the chromosphere and transition region line fluxes may have been produced by

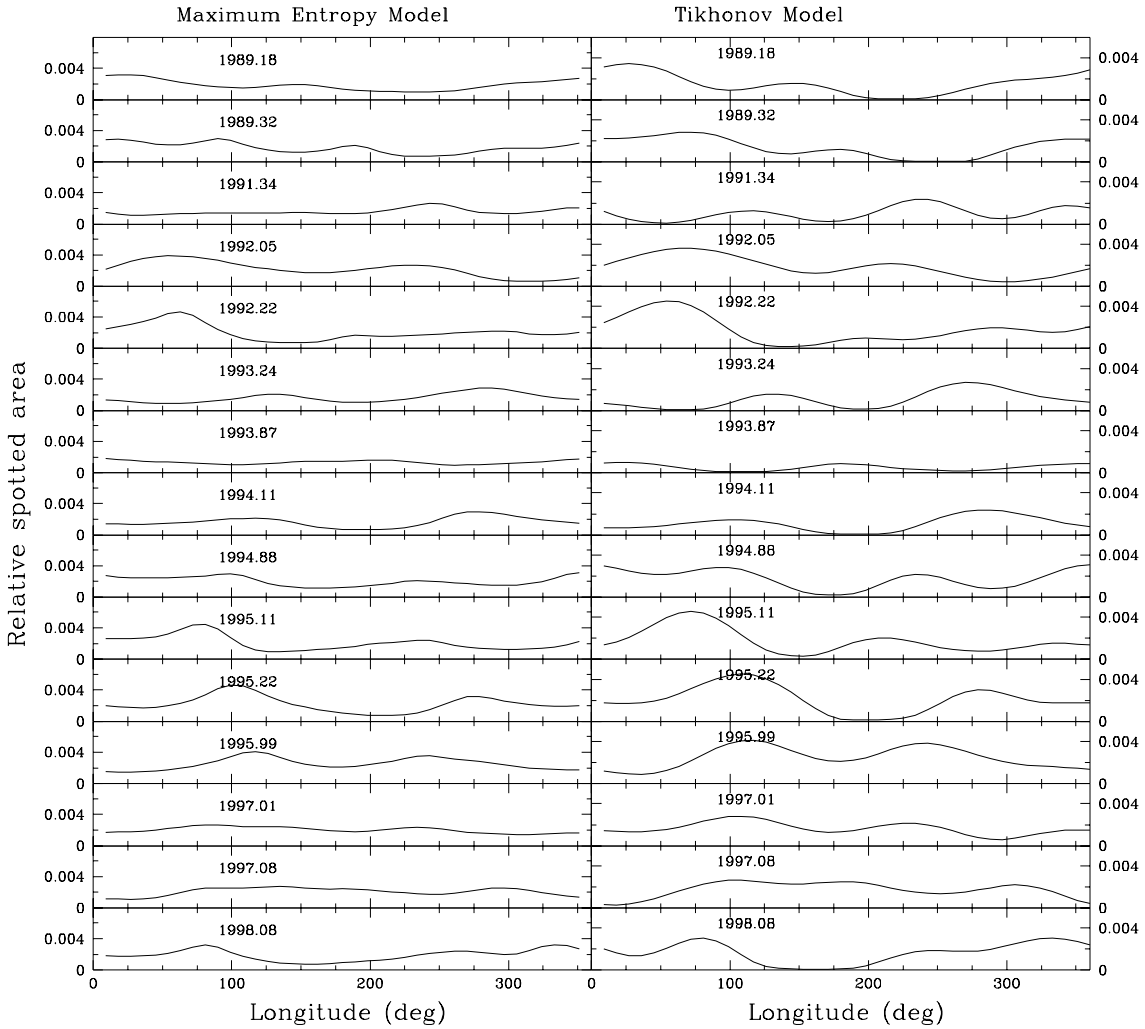

Fig. 5. The distribution of the relative spotted area vs. longitude for the light curves from 1989.18 to 1998.08 obtained from the Maximum Entropy models (*left panels*) and the Tikhonov models (*right panels*). The area unit is the photospheric area of the star.

a temporary enhancement of the emission of the upper atmosphere due to the occurrence of a flare at the same phase of the previously mentioned optical flare observed during the 1992.05 light curve. Unfortunately the time span of the IUE observations covers only one rotation of HD 82443, which makes it impossible to distinguish between rotational modulation and intrinsic variation of the line fluxes.

The available data on the long-term changes of the chromospheric and transition region emissions, also reported in Table 3, show a rather constant level of activity within 10–20%, but again a more extended data sequence is needed to derive certain conclusions.

5. Discussion

The above results allow us to deduce some general characteristics of the magnetic activity of HD 82443, comparing also its behaviour with that observed in the Sun.

The overall activity level, measured by the total spot coverage, displays a short-term cyclic modulation with a mean period of $P_{cyc} = 3.89$ yr. Such a result is certainly significant not only because of the low level of the false-alarm-probability, but also because more than two cycles are covered by the observations.

The period of the activity cycle of HD 82443 is significantly shorter than the 11-yr solar cycle, but it is in fairly good agreement with the general trend found by Baliunas et al. (1996b) for lower main-sequence stars for which long-term records of the Ca II fluxes are available.

The seasonal changes of the photometric period may be explained in terms of a migration of the activity belts over the surface of a differentially rotating star, as observed on the Sun (cf. Donahue & Keil 1995). However, it is not possible to confirm directly such a hypothesis because the stellar disk is not resolved and the latitudes of the spots obtained by modelling the photometric data are highly uncertain. It is important to note that, in addition to the change of the spot rotation period, a factor which may produce variations of the photometric period is the growth and decay of the starspots. Dobson et al. (1990), Donahue & Baliunas (1992) and Donahue (1993) have proposed a method to estimate the effect of the active region

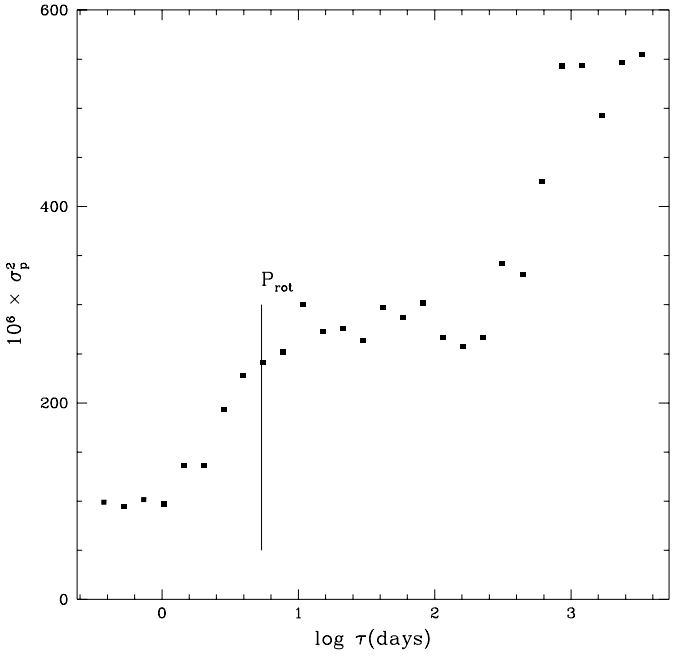

Fig. 6. The variance profile of HD 82443 vs. the time scale τ. The time scale corresponding to the mean photometric period P_{rot} is indicated by the vertical dash.

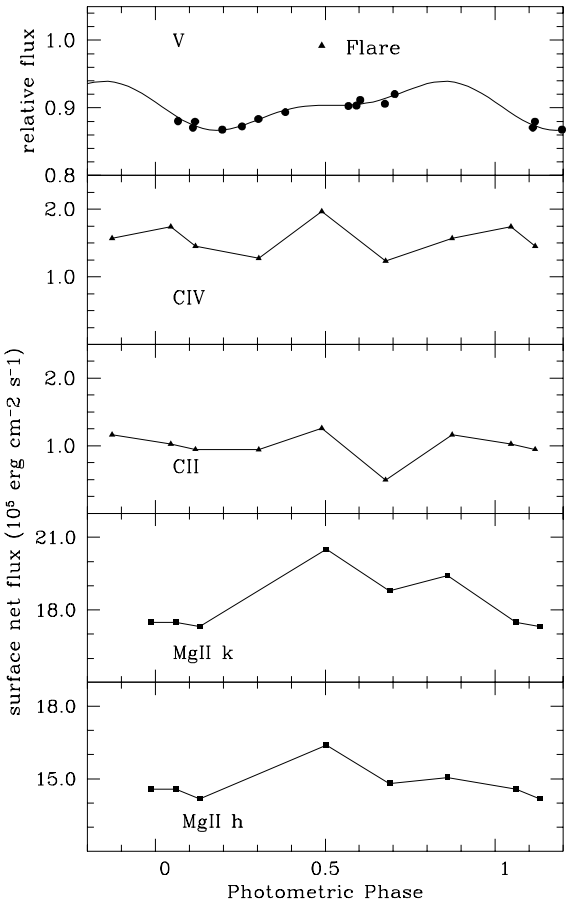

Fig. 7. Simultaneous variations (*lower panels*) of the integrated surface net fluxes of several chromospheric and transition region UV lines vs. photometric phase computed according to Eq. (1). The 1992.05 V-band light curve is plotted for comparison (*top panel*), including the normal point corresponding to the white light flare observed around phase 0.49 and previously neglected in the light curve modelling.

evolution based on the analysis of the variance present in the photometric time series over different time scales, the so-called *pooled variance analysis*.

The variance profile for the photometric data set of HD 82443 has been computed following the prescription by Donahue (1993) and has been plotted in Fig. 6. The mean semi-amplitude of the sinusoidal fits to the observed flux modulation is $A_{ave} = 0.021$ mag. The difference between the pooled variance computed at the time scale of rotation, $\sigma^2_{rot} \simeq 3\times10^{-4}$ and the variance at the shortest measurable time scale $\sigma^2_{base} \simeq 10^{-4}$, gives a semi-amplitude $A_p = \sqrt{\sigma^2_{rot} - \sigma^2_{base}} \simeq 0.014$, indicating that $\sim 70\%$ of the variance observed at the rotation period is associated with the rotational modulation of the optical flux. The observed variance for time scales longer than the rotation period levels off and begins to increase significantly only at $\log\tau \simeq 2.2$, ($\tau \simeq 160$ days) which corresponds to the time scale of the active region evolution estimated with the starspot models. Therefore, the interpretation of the changes of the photometric period of HD 82443 in terms of a variation of the rotation period of the starspots appears to be the most likely explanation, also in consideration of the comparable results obtained for the Sun (cf. Donahue & Keil 1995). However, the variation of the spot rotation period of HD 82443 versus the phase of the activity cycle is at variance with the behaviour observed in the Sun, because it increases with the cycle phase. Such a behaviour has been observed in two other chromospherically active stars: HD 114710 and HD 10476 (Donahue & Baliunas 1992, Donahue 1996) and, in the absence of any latitudinally resolved map, it is only possible to speculate about its possible causes.

In the Sun the migration of the active regions is regarded as a consequence of the latitudinal migration of a dynamo wave propagating in a shell near the base of the solar convection zone. The direction of migration is related to the sign of the product of the radial gradient of the angular velocity in the shell $\frac{\partial\Omega}{\partial r}$ by the parameter α, which measures the intensity of the regeneration of the poloidal field component by cyclonic convection (Moffatt 1978)[2]. In the Sun the sign of $\alpha\frac{\partial\Omega}{\partial r}$, at low and intermediate latitudes, is such as to produce an equatorialward migration of the dynamo wave (Stix 1976). Such a migration, in association with the increase of the angular velocity toward the equator ($\frac{\partial\Omega}{\partial\phi} < 0$, where ϕ is the latitude), is responsible for the decrease of the rotation period of the active regions of the Sun versus increasing cycle phase. Although a different pattern of the differential rotation (or of the α effect) might be invoked to explain the behaviour of HD 82443, it is also possible to propose an interpretation in terms of high latitude starspot activity with the same internal differential rotation pattern of the Sun. Specifically, helioseismic observations show that the radial gradient at

[2] In the present discussion we shall assume that any possible meridional flow does not affect significantly the migration of the dynamo wave in the Sun and active stars.

the base of the convection zone $\frac{\partial\Omega}{\partial r}$ changes sign for $\phi > 40°$ (e.g., Kosovichev 1996). The solar dynamo is not strong enough to produce spot activity at latitudes $\phi > 40°$, but in more active stars the dynamo may be expected to amplify significantly the toroidal field up to subpolar latitudes (e.g., Tobias et al. 1997, Belvedere et al. 1998). The high latitude spot belts ($\phi > 40°$) will migrate toward the pole, because the sign of $\alpha\frac{\partial\Omega}{\partial r}$ is opposite to that in the low latitudes ($\phi < 40°$), and if the rotation axis of the star is inclined with respect to the line of sight, the high latitude spots may well dominate the optical modulation producing an increase of the photometric period with the activity cycle phase.

6. Conclusion

The analysis of a long-term sequence of optical light curves of HD 82443 adopting the Maximum Entropy and Tikhonov regularization criteria has revealed several characteristics of the magnetic activity of that young, main-sequence star. An extended spot pattern is present on its photosphere showing changes of the total area as large as $\sim 10\%$ of the star's surface along a mean activity cycle of 3.89 yr. The evidence for such a short-term cycle is quite compelling since the present data cover more than two complete cycles. Moreover, the photometric period appears to be correlated with the phase of the activity cycle with the spot rotation period increasing with the cycle phase. Such a behaviour, which is opposite to that observed in the Sun, has been previously found in HD 114710 and HD 10476 and may possible be evidence for high latitude activity or an internal differential rotation different from the solar one. Unfortunately, we have no reliable information on the latitude of the spots from photometric models and therefore it is not possible to test the proposed explanations. Only a lower limit for the amplitude of the surface differential rotation can be derived for HD 82443, $\Delta\Omega/\Omega \simeq 0.04$ which is lower than solar, but in fairly good agreement with the values found by Henry et al. (1995b) for a quite large sample of active stars.

Future systematic and continuous observations of HD 82443 will be useful to confirm whether the rotation periods accurately describe a pattern which is opposite to that of the Sun. If the proposed scenario will be confirmed, we expect a sudden reduction of the photometric period in the near future as the next activity cycle will begin, followed by a steady increase during its progress. Unfortunately, the low value of the rotational line broadening makes it very difficult to obtain Doppler images of HD 82443, preventing us from determining the direction of migration of the spots in latitude and the sign of the surface gradient of the differential rotation.

Data on the chromospheric and transition region line fluxes have also been discussed in the present study and the spatial association between photospheric spots and plages in the outer atmosphere has been addressed, but more extended and simultaneous optical and UV observations are needed for an assessment of such an aspect of the star's activity.

Acknowledgements. The authors are grateful to one of the Referees, Dr. G. W. Henry, for pointing out a problem in the reduction of the photometric data presented in a previous version of the present paper and for his stimulating comments. We are also grateful to Dr. R. Ventura for providing us with the periodogram analysis code. Active star research at Institute of Astronomy of Catania University and Catania Astrophysical Observatory is funded by MURST (*Ministero dell'Università e della Ricerca Scientifica e Tecnologica*), CNAA (*Consorzio Nazionale per l'Astronomia e l'Astrofisica*) and the *Regione Siciliana*, whose financial support is gratefully acknowledged.

References

Baliunas S.L., Donahue R.A., Soon W.H., et al., 1995, ApJ 438, 269
Baliunas S.L., Sokoloff D., Soon W.H., 1996a, ApJ 457, L99
Baliunas S.L., Nesme-Ribes E., Sokoloff D., Soon W.H., 1996b, ApJ 460, 848
Barnes T.G., Evans D.S., 1976, MNRAS 174, 489
Belvedere G., Lanza A.F., Sokoloff D., 1998, Sol. Phys. 183, 435
Benz W., Mayor M., 1984, A&A 138, 183
Boyd L., Genet R.M., 1986, PASP 98, 618
Cameron A.C., 1992, In: Byrne P.B., Mullan D.J. (eds.) Surface Inhomogeneities on Late-Type Stars. Springer-Verlag, Berlin, p. 33
Díaz-Cordovés J., Claret A., Giménez A., 1995, A&AS 110, 329
Dobson A.K., Donahue R.A., Radick R.R., Kadlec K.L., 1990, In: Wallerstein G. (ed.) The Sixth Cambridge Symposium on Cool Stars, Stellar Systems and the Sun. ASP Conf. Ser. vol. 9, p. 132
Donahue R.A., 1993, Ph.D. Thesis, New Mexico State University
Donahue R.A., 1996, In: Strassmeier K., Linsky J.L. (eds.) IAU Symp. 176, Stellar Surface Structures. Kluwer, Dordrecht, p. 261
Donahue R.A., Baliunas S.L., 1992, ApJ 393, L63
Donahue R.A., Keil S.L., 1995, Sol. Phys. 159, 53
Duquennoy A., Mayor M., Halbwachs J.L., 1991, A&AS 88, 281
Fekel F.C., 1997, PASP 109, 514
Griffin R.F., 1994, The Observatory 114, 294
Henry G.W., Fekel F.C., Hall D.S., 1995a, AJ 110, 2926
Henry G.W., Eaton J.A., Hamer J., Hall D.S., 1995b, ApJS 97, 513
Horne J.H., Baliunas S.L., 1986, ApJ 302, 757
Kazarovets E.V., Samus N.N., 1997, IBVS 4471
Kopal Z., 1959, Close Binary Systems. Chapman & Hall, London
Kosovichev A.G., 1996, ApJ 469, L61
Lampton M., Lieu R., Schmitt J.H.M.M., et al., 1997, ApJS 108, 545
Lanza A.F., Catalano S., Cutispoto G., Pagano I., Rodonò M., 1998, A&A 332, 541
Messina S., Guinan F.E., 1996, IBVS 4286
Moffatt H.K., 1978, Magnetic Field Generation in Electrically Conducting Fluids. Cambridge Univ. Press, Cambridge
Perryman M.A.C., 1997, The Hipparcos and Tycho Catalogues, ESA publications SP-1200
Scargle J.D., 1982, ApJ 263, 835
Soderblom D.R., 1985, AJ 90, 2103
Soderblom D.R., 1995, priv. commun.
Soderblom D.R., Clements S.D., 1987, AJ 93, 920
Stix M., 1976, A&A 47, 243
Strassmeier K.G., Bartus J., Cutispoto G., Rodonò M., 1997, A&AS 125, 11
Teays T.J., Garhart M.P., 1990, IUE Newsletter 41, 94
Tobias S.M., Proctor M.R.E., Knobloch E., 1997, A&A 318, L55